JOURNAL OF CATALYSIS **159,** 353–360 (1996)
ARTICLE NO. 0097

Influence of Zeolite Composition and Structure on Hydrogen Transfer Reactions from Hydrocarbons and from Hydrogen

Josefin Meusinger* and Avelino Corma†

**Institute of Chemical Technology, Department of Chemistry, University of Leipzig, Linnèstrasse 3, 04103 Leipzig, Germany; and*
†Instituto de Tecnología Química, UPS-CSIC, Universidad Politécnica de Valencia, Avenida de los Naranjos s/n, 46022 Valencia, Spain

Received March 7, 1995; revised November 17, 1995; accepted November 24, 1995

The cracking of *n*-heptane proceeds at 623 K and a reaction pressure of 2.5 MPa preferentially according to the bimolecular cracking route. This was confirmed for MFI- and FAU-type zeolites with varying density of acid sites. The activity was found to be linearly dependent on the number of Brønsted acid sites for MFI-type zeolites. In the case of FAU-type zeolites it was observed that the activity per Brønsted acid site decreases with increasing concentration of acid sites. This was explained by differences in acid strength. All the investigated acid zeolite samples were able to activate hydrogen under the actual reaction conditions. The activated hydrogen was found to participate in bimolecular hydrogen transfer reactions during *n*-heptane cracking. The action of hydrogen is discussed on the basis of its influence on the rate-determining step during cracking and was confirmed by a kinetic study of *n*-heptane cracking on a FAU-type sample. Hydrogen transfer from hydrogen as well as from hydrocarbons was influenced in the same way by zeolite structure and acid site density.

INTRODUCTION

The cracking of *n*-alkanes can proceed via a bimolecular or a monomolecular reaction pathway (1). There are several studies dealing with the relation between the properties and performance of zeolites in *n*-alkane cracking. Haag and Dessau (1) found that the monomolecular protolytic route is more favored with the medium-pore zeolite ZSM-5 (MFI) than with a large-pore Y zeolite (FAU). Furthermore, they have shown that bimolecular cracking becomes the prominent pathway with decreasing temperature and increasing partial pressures of the hydrocarbon.

Giannetto *et al.* (2) concluded that classical bimolecular cracking is more pronounced with an aluminium-rich FAU sample than with a silicon-rich FAU sample. Mirodatos and Barthomeuf (3) suggested that protolytic cracking is favored with small-pore zeolites and/or zeolites with a high tortuosity. Wielers *et al.* (4) confirmed these results and have shown that with increasing temperature, decreasing aluminium content, and decreasing pore dimensions the relative contribution of the monomolecular protolytic cracking route increases as compared to bimolecular cracking.

When performing *n*-heptane cracking with an HZSM-5 zeolite at a reaction temperature of 543 K and a total reaction pressure of 2.4 MPa (5), it appeared that the reaction follows preferentially the bimolecular pathway, which means that the reaction chain is propagating via bimolecular hydride abstraction from an alkane molecule and its transfer to an intermediate carbenium ion. In this previous work it was shown that under these reaction conditions the cracking rate was controlled by the rate of desorption of reaction products. Thus, the introduction of hydrogen into this system causes an increase of the initial rate of cracking, which was explained by assuming that hydrogen interacts with adsorbed olefins, hydrogenates them, and forces their desorption. The hydrogenation produces saturated molecules in competition with the bimolecular hydride abstraction from hydrocarbons. In both reactions hydrogen is transferred to adsorbed unsaturated molecules.

Whereas there is much information concerning hydrogen transfer between hydrocarbons, there is a lack of information concerning hydrogen transfer with molecular hydrogen. In this work we have investigated the role of zeolite structure and acid site density on hydrogen transfer reactions involving *n*-heptane and molecular hydrogen during *n*-heptane cracking.

EXPERIMENTAL

Preparation and Characterization of Catalysts

HZSM-5 samples with different Si/Al ratios were synthesized template-free and were activated by ammonium exchange and calcination (6). The Si/Al ratio of the modified zeolites was determined by chemical analysis.

Sample FAU1 with a unit cell size of 2.448 nm was obtained by steam calcination at 873 K and 100% steam of a partially ammonium-exchanged NaY zeolite (Linde SK 40), followed by ammonium exchange. Sample FAU2 was prepared by steam calcination of FAU1 at 923 K, followed

0021-9517/96 $18.00

by ammonium exchange. Portions of these samples were treated with a 0.4 *M* solution of $(NH_4)_2SiF_6$ at 363 K for 3 h. This treatment was done with $(NH_4)_2SiF_6$-to-zeolite ratios of 0.26 g g^{-1} (FAU1 → FAU1F1, FAU2 → FAU2F) and 0.47 g g^{-1} (FAU1 → FAU1F2).

The unit cell size of the final USY zeolites was determined by X-ray diffraction using Cu$K\alpha$ radiation and following ASTM procedure D-3942-80. The estimated standard deviation was 0.001 nm. The crystallinity of these samples was calculated by comparing the peak height of the (5, 3, 3) reflection and considering the reference NaY SK-40 as presenting 100% crystallinity. The Si/Al (XRD) ratio for the samples was calculated on the basis of the Fichtner-Schmittler equation (7). The differences between these values and those obtained by chemical analysis (Si/Al (chem)) allowed us to calculate the amount of Al in extraframework positions (EFAL).

The IR spectroscopic measurements were carried out in a conventional greaseless IR cell. Wafers of 10 mg cm^{-2} were pretreated overnight at 673 K and 10^{-3} MPa dynamic vacuum. The spectra in the 4000–1300 cm^{-1} region were recorded at room temperature in a Perkin–Elmer 580 B spectrometer equipped with a data station. For pyridine adsorption experiments 6.66×10^2 Pa of pyridine were introduced into the cell at room temperature. After equilibration, the samples were outgassed at 523, 623, and 673 K under vacuum and the spectra were recorded at room temperature. Intensities of the bands at 1540 cm^{-1} (Brønsted sites) and 1450 cm^{-1} (Lewis sites) and apparent extinction coefficients reported by Emeis (8) were used to determine the concentration of acid centers.

Furthermore, the BET surface area and the micropore volume of the FAU-type samples were determined by adsorption of nitrogen at 77 K in an ASAP 2000 instrument.

Catalytic Experiments

The reactions have been carried out in a stainless steel tubular reactor whose inner surface was passivated by graphitation. The details are described elsewhere (5). Performing blank experiments with *n*-heptane ($p_{n\text{-heptane}}$, 0.4 MPa) and 1-butene ($p_{1\text{-butene}}$, 0.02 MPa)it was verified that there was no conversion of the alkane and not more than 3% of the olefin was converted. The reaction was studied at 623 K and a total pressure of reaction of 2.4 MPa. The *n*-heptane flow was chosen in the range between 0.35 and 0.39 ml min^{-1}. If not indicated otherwise, the ratio of *n*-heptane to the diluting gas was kept constant at 0.18 mol mol^{-1}. Nitrogen or hydrogen or mixtures of both gases were taken as diluting gases. The zeolites have been used as pressed powders with a mesh size between 0.25 and 0.42 mm. The amount of catalyst was varied between 0.15 and 0.45 g.

Sample MFI1 was used to check that under these conditions the reaction is not controlled by external diffusion. To examine the relevance of internal mass transfer, experiments with different mesh sizes (MFI1) were carried out and no significant influence on reaction rate was observed in the chosen range of mesh sizes.

The reaction was always followed at different times-on-stream (TOS) starting at 0.5 min TOS. It was supposed that at this short TOS the influence of deactivation was negligible. The activity of the different zeolites for cracking *n*-heptane under these reaction conditions was expressed by the conversion. The reaction kinetics were determined at levels of conversion below 10% and then the cracking rate was calculated from the rates of formation of hydrocarbons with one to six carbon atoms, i.e., cracking rate $= 1/7(r_{C_1} + 2r_{C_2} + 3r_{C_3} + 4r_{C_4} + 5r_{C_5} + 6r_{C_6})$, where the values of r_{C_i} represent the rate of formation of a hydrocarbon with *i* carbon atoms, the dimensions of the rate being mol g^{-1} min^{-1}.

RESULTS AND DISCUSSION

Physico-Chemical Properties of Used Zeolites

In Tables 1 and 2 the physico-chemical properties of the zeolite samples derived from the methods applied are given. In the case of MFI-type zeolites the synthesis products were checked by XRD and all samples were identified as pure and highly crystalline ZSM-5 zeolite. A characteristic IR spectrum of sample MFI1 after pyridine adsorption is given in Fig. 1 and the low intensity of the band at 1450 cm^{-1} was taken as evidence that the number of extraframework aluminium species (EFAL) was negligible. Therefore, it was assumed that nearly all of the aluminium was located on framework positions (FAL). Taking this into account, the values obtained from the chemical analysis were used to calculate the Al/(Al + Si) ratios given in Table 1. The concentrations of Brønsted acid sites were calculated from IR spectra recorded after outgassing the pyridine-loaded samples at 523 K (Table 1). From the Al/(Al + Si) ratios of the MFI samples, it is possible to assume that all the framework Al is isolated and the associated acid sites should be equivalent. Therefore, differences in the catalytic activity

TABLE 1

Physico-Chemical Properties of MFI-Type Zeolites

	MFI1	MFI2	MFI3
Si/Al (chem)	15.5	22.8	24.0
Al/(Al + Si)	0.060	0.042	0.040
C_B (μmol g^{-1})	104	94	92
C_L (μmol g^{-1})	7	6	9
C_B/C_L	14.8	15.7	10.2

TABLE 2

Physico-Chemical Properties of FAU-Type Zeolites

	FAU1	FAU1F1	FAU1F2	FAU2	FAU2F
a_0 (nm)	2.448	2.447	2.439	2.433	2.434
Crystallinity (%)	100	90	74	92	71
Si/Al (XRD)	5.9	6	9.9	16.6	15
Si/Al (chem)	3.7	12.1	4.1	8.6	6.6
FAL/u.c.	28	27	18	11	12
EFAL/u.c.	16	2	3	34	9
Al/(Al + Si)	0.1447	0.1428	0.0920	0.0568	0.0625
C_B (μmol g^{-1})	97	154	85	12	41
C_L (μmol g^{-1})	26	8	16	13	19
C_B/C_L	3.7	19.2	5.5	0.9	2.2
$V_{micropore}$ (ml g^{-1})	0.1954	0.2269	0.1854	0.2045	0.1609

should be related to differences in the number of sites (9) rather than to their acid strength.

In Table 2 the total amount of FAL and EFAL and other physico-chemical properties of the FAU-type zeolite samples are summarized. The pretreatment of sample FAU1 and sample FAU2 with $(NH_4)_2SiF_6$ causes the removal of EFAL (10) while the framework composition remains practically the same. This is supported by the low value of extraframework species in the samples FAU1F1 and FAU2F calculated from chemical analysis and the unit cell parameters, as well as by the small number of Lewis acid sites derived from the IR spectroscopy. By increasing the concentration of the $(NH_4)_2SiF_6$ it was possible to remove not only most of the EFAL but also framework Al, producing a further dealuminated almost EFAL-free Y zeolite (FAU1F2). The hydrothermal pretreatment, and especially the EFAL extraction, produces a decrease in zeolite crystallinity. Comparing the composition of sample FAU1 with FAU1F1 and FAU2 with FAU2F one can see that the removal of EFAL results in an increase in the amount of Brønsted acid sites measured by pyridine adsorption/desorption. This can be explained by assuming that cationic EFAL species partly compensate the negative charge of the anionic zeolite framework and/or that these species are deposited in the channels of the zeolite, blocking the access of pyridine to acid hydroxyl groups related to the framework aluminium (10). The decrease in the micropore volume of sample FAUF2 in comparison to FAU2 should be attributed to the loss in crystallinity (Table 2). These results indicate that USY zeolites are characterized by more complex acidic properties. A direct correlation between catalytic activity and framework Al content should not necessarily be expected. Furthermore, the samples containing more than 35–25 Al per unit cell may have Brønsted acid sites with lower acid strength than samples with lower Al contents (11).

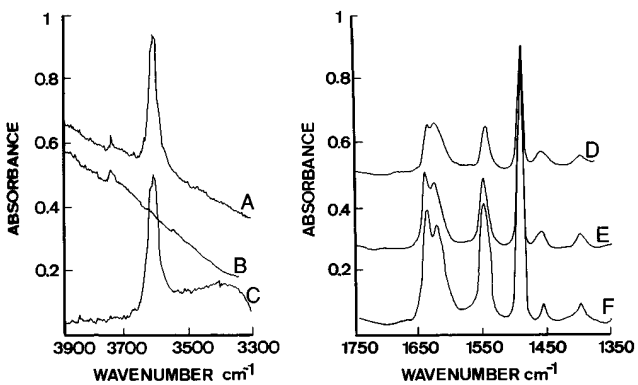

FIG. 1. Infrared spectra of sample MFI1 activated in ultrahigh vacuum at 673 K (A), after adsorption of pyridine and outgassing at 523 K (B). Difference spectra of A and B (C); difference IR spectra of sample MFI1 after adsorption of pyridine and outgassing at 673 K at 673 (D), 623 (E), and 523 K (F).

Hydrogen Transfer during n-Heptane Cracking in Nitrogen Atmosphere

The product distribution and selectivities obtained during *n*-heptane cracking on MFI zeolites are given in Table 3. From these results it becomes clear that despite possible differences due to the different levels of conversion the product distribution with respect to the C-number of cracking products reflects an excess in the formation of C_5 and C_6 hydrocarbons in comparison to C_1 and C_2 hydrocarbons. This can be rationalized by assuming that besides the direct cracking events, which give C_3/C_4, C_2/C_5 and C_1/C_6 in equal amounts, further reactions have taken place. In a previous work (12) a stoichiometric network including dimerization steps was derived in order to explain the unbalance in light cracking products during *n*-heptane cracking at 543 K. In the present work the high hydrocarbon partial pressure and the relatively low temperature permit the occurrence of dimerization-cracking reactions in the medium pore size MFI zeolite. Thus, it is not surprising that under these conditions a large contribution to the bimolecular cracking route may exist in the case of MFI zeolites. Indeed, when the relative contribution of the monomolecular to the bimolecular cracking mechanism has been calculated from the $(C_1 + C_2)$ to isobutane ratio (cracking mechanism ratio, CMR) (4), it can be seen that the ratio is much lower than one. As expected, the CMR value decreases when the *n*-heptane partial pressure increases (Fig. 2).

Furthermore, the paraffin to olefin ratio (*P/O*) can be taken as a yardstick for hydrogen transfer reactions (13) and can be interpreted as the average chain length (repetition of hydrogen transfer steps). It can be expected that this value behaves sensitively to variations in the conversion, zeolite composition, and zeolitic geometry. The molar ratio of paraffins to olefins (*P/O*) was examined for different levels of conversion for sample MFI1. The results given in Fig. 3 clearly indicate an increase of the *P/O* ratio with increasing conversion. Therefore, the slightly higher

TABLE 3

Product Distribution and Selectivities during *n*-Heptane Cracking on MFI-Type Zeolites

	MFI1		MFI2		MFI3	
	N_2	H_2	N_2	H_2	N_2	H_2
Conversion at 0.5 min TOS (mol%)	62.7	93.1	49.2	84.6	47.5	84.5
C_1	0.12	0.74	0.09	0.60	0.12	0.63
C_2	1.04	1.72	1.14	1.51	1.18	1.48
C_3	41.64	43.20	41.12	40.58	41.97	41.62
C_4	37.09	36.39	38.43	36.96	37.88	37.07
C_5	12.87	12.95	14.48	14.61	13.89	14.04
C_6	7.24	4.99	4.74	5.74	4.96	5.16
$S_{isomerization}$	1.95	2.15	3.09	2.75	2.14	2.65
iC_4/nC_4	0.84	0.89	0.74	0.83	0.75	0.88
P/O	8.6	40.3	7.6	23.0	7.2	25.8
CMR $= (C_1+C_2)/iC_4$	0.05	0.06	0.06	0.06	0.04	0.06

values of the *P/O* ratio observed with increasing number of FAL in MFI type zeolites should rather be related to the higher total conversion than to changes in the properties of the zeolite samples. In general, the observed values of the *P/O* ratio at 0.5 TOS underline the importance of the bimolecular hydride transfer reactions during cracking under the given reaction conditions with all the investigated MFI zeolites.

Analyzing the product distribution for *n*-heptane cracking on FAU-type zeolites, one can conclude that the process is characterized by bimolecular cracking events and includes steps of dimerization just as was shown to occur for the medium-pore zeolites (Table 4). Furthermore, the values for the cracking mechanism ratio and the ratio of isobutane to *n*-butane also support this statement (Table 4).

Regardless of the zeolite type used, the cracking of *n*-heptane seems to be characterized preferentially by bimolecular cracking under the given experimental conditions. However, comparing the results from Tables 3 and 4, it becomes clear that an increase in the pore dimensions of the zeolite increases the relative contribution of the bimolecular versus the monomolecular reaction pathway. This can be deduced from the lower values of the CMR as well as from the higher *P/O* ratio found with USY than with MFI zeolites.

Hydrogen Transfer Involving Molecular Hydrogen during n-Heptane Cracking

In previous papers (5, 12) it has been shown that hydrogen can become activated on acid HZSM-5 zeolite

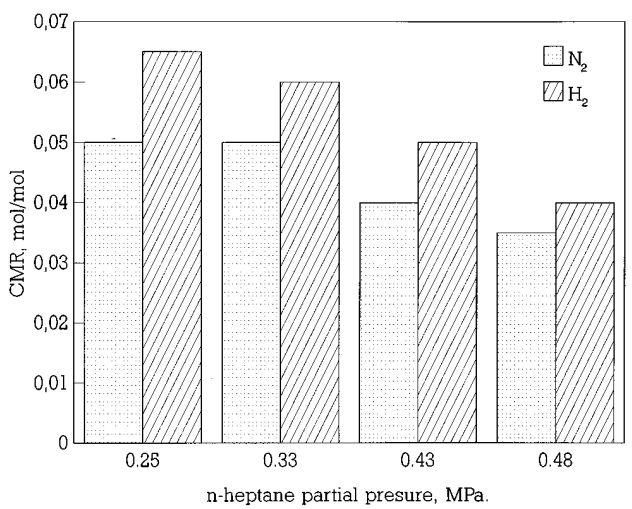

FIG. 2. Cracking mechanism ratio (CMR) dependent on the *n*-heptane partial pressure during *n*-heptane cracking in nitrogen atmosphere on sample MFI1; temperature, 543 K; p_{total}, 2.4 MPa.

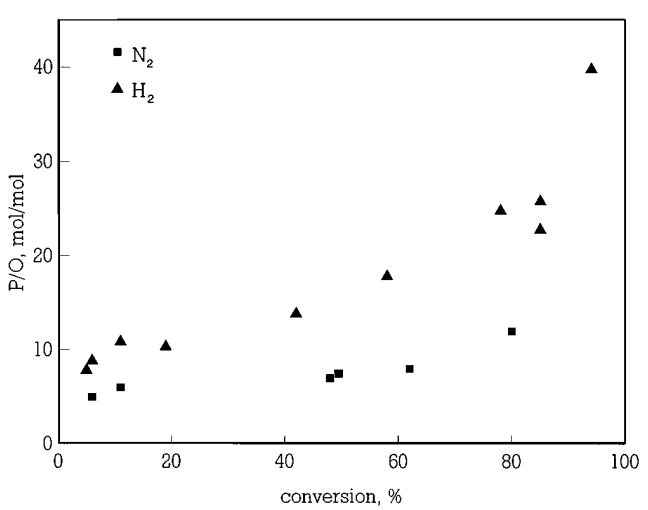

FIG. 3. Molar ratio of paraffins to olefins formed during *n*-heptane cracking on sample MFI1 dependent on conversion: temperature, 623 K; p_{total}, 2.4 MPa; $p_{n\text{-heptane}}$, 0.4 MPa.

TABLE 4

Product Distribution and Selectivities during *n*-Heptane Cracking on FAU-Type Zeolites

	FAU1		FAU1F1		FAU1F2		FAU2		FAU2F	
	N_2	H_2	N_2	H_2	N_2	H_2	N_2	H_2	N_2	H_2
Conversion at 0.5 min TOS (mol%)	20.4	33.3	21.8	33.6	21.3	32.7	19.1	22.5	23.0	26.2
C_1	0.34	0.16	0.04	0.09	0.05	0.07	0	0	0.32	0.13
C_2	0.74	0.85	0.45	0.72	0.48	0.92	1.07	0.53	0.38	0.62
C_3	40.34	41.31	39.11	39.25	40.77	41.38	41.80	43.45	39.00	39.39
C_4	45.96	45.88	46.99	46.72	45.56	45.10	46.96	43.41	47.03	46.89
C_5	8.67	8.02	9.14	8.76	8.51	7.98	6.26	6.72	8.86	8.56
C_6	3.95	3.78	4.27	4.46	4.63	4.55	3.91	5.89	4.41	4.41
$S_{isomerization}$	9.4	11.1	9.7	9.9	8.73	8.96	16.0	16.4	7.9	8.8
iC_4/nC_4	5.21	5.44	5.74	5.93	5.43	5.89	6.26	6.42	6.26	6.42
P/O	22.95	29.6	32.6	35.7	21.3	29.9	20.1	24.5	28.8	33.5
$CMR = (C_1 + C_2)/iC_4$	0.03	0.03	0.01	0.02	0.03	0.03	0.02	0.02	0.02	0.02

and intervenes in acid-catalyzed cracking reactions. To explain the experimental results the following reactions were proposed to occur (12). An olefin $[C_nH_{2n}]$ interacts with a Brønsted site to form an adsorbed carbenium ion $[C_nH_{2n}H^+(ads)]$. Surface reaction (1) proceeds between this ion and an educt paraffin molecule $[C_mH_{2m+2}]$ such that via hydride abstraction a paraffinic product molecule $[C_nH_{2n+2}]$ and a long-chain carbenium ion $[C_mH_{2m}H^+(ads)]$ are formed:

$$C_nH_{2n}H^+(ads) + C_mH_{2m+2} \rightarrow C_mH_{2m}H^+(ads) + C_nH_{2n+2}. \quad [1]$$

Then, β-scission (reaction (2)) of $C_mH_{2m}H^+(ads)$ leads to the formation of an olefin $[C_iH_{2i}]$ and a further carbenium ion $[C_jH_{2j}H^+(ads)]$ which remains at the surface:

$$C_mH_{2m}H^+(ads) \rightarrow C_iH_{ij} + C_jH_{2j}H^+(ads). \quad [2]$$

The final step of the process is the desorption (reaction [3a]) of an olefin $[C_jH_{2j}]$ from $C_jH_{2j}H^+(ads)$:

$$C_jH_{2j}H^+(ads) \rightarrow C_jH_{2j} + H^+(ads). \quad [3a]$$

If hydrogen is present in the reaction mixture desorption can be promoted by the hydrogen molecule (reaction [3b]) forming a paraffin:

$$C_jH_{2j}H^+(ads) + H_2 \rightarrow C_jH_{2j+2} + H^+(ads). \quad [3b]$$

It was demonstrated that hydride abstraction can occur from hydrocarbons [1] and molecular hydrogen [3b], and both reactions are competing. The latter promotes the desorption of olefinic reaction products and restoration of the former occupied Brønsted acid site. Hence, the presence of hydrogen can increase the cracking activity in cases where the desorption of olefinic products is the rate-determining step. However, if hydride abstraction (1) is the slowest step of the global process, this hydrogenation diminishes the concentration of reactive intermediates and a rate-promoting effect of hydrogen seems to be unlikely. This is indeed observed (Fig. 4) when the cracking of *n*-heptane was carried out on a USY zeolite (FAU1). At low partial pressures of the hydrocarbon the presence of hydrogen practically does not affect the rate of reaction, while at higher partial pressures where the reaction is already of zero order, the introduction of hydrogen causes not only an increase in the reaction rate, but a change in the nature of the controlling step of the reaction.

If the nature of this hydrogenation reaction [3b] is similar to "normal" hydrogen transfer (for instance, that described above in reaction [1]) similar rules should be valid concerning its sensitivity to zeolitic properties. Thus, by performing the cracking of *n*-heptane in hydrogen atmosphere

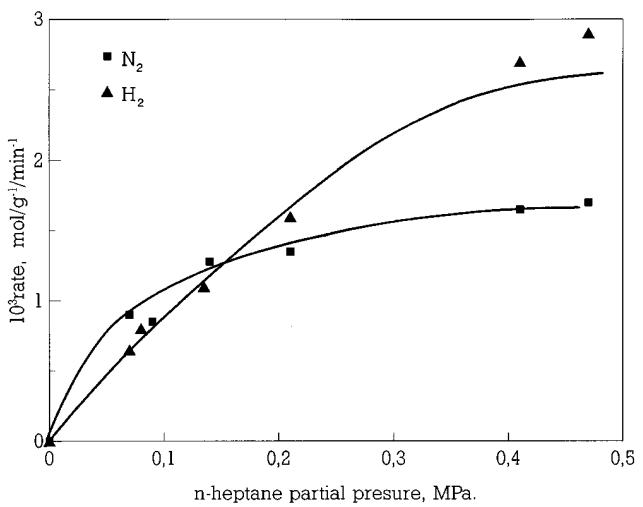

FIG. 4. Cracking rate dependent on *n*-heptane partial pressure on sample FAU1: temperature, 623 K; p_{total}, 2.4 MPa.

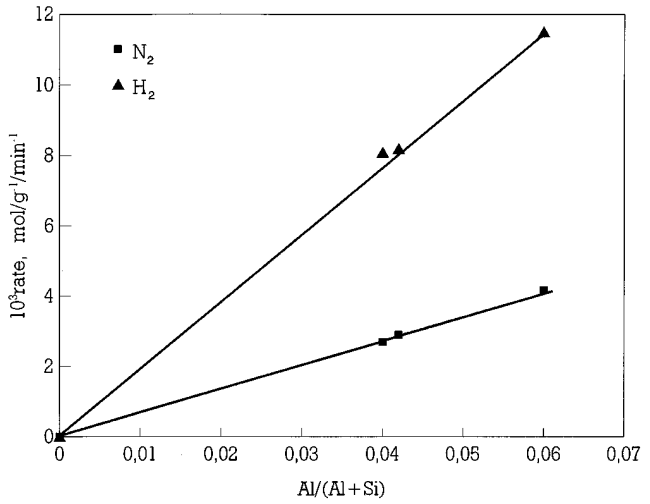

FIG. 5. Cracking rate of MFI-type zeolites dependent on aluminium content of the zeolite: temperature, 623 K; p_{total}, 2.4 MPa; $p_{n\text{-heptane}}$; 0.4 MPa.

with different zeolite types and zeolites with varying concentrations of acid sites we can expect to confirm the common validity of hydrogen transfer reactions from molecular hydrogen and should obtain information about the influence of zeolitic properties for hydrogen activation, the rate-determining step during cracking, and the reactivity of intermediates.

Increasing the number of Brønsted acid sites in MFI-type zeolites results in a proportional increase of the cracking activity in nitrogen atmosphere (Fig. 5). Substitution of nitrogen by hydrogen produces an enhancement of cracking activity, and a linear correlation (but with a higher slope) is again found between activity and the concentration of Brønsted acid sites (Fig. 5). According to our previously reported data, this result concerning the hydrogen influence can be interpreted in the following way. Desorption of reaction products is the rate-determining step with MFI zeolites [3a]. If the intrinsic concentration of these intermediates is high enough to cover all the available sites, the reaction is inhibited by the reaction products adsorbed on Brønsted acid sites. This presupposes that the desorption of unsaturated adsorbed hydrocarbons is slower than the steps propagating the reaction chain. This undesired effect can be counteracted via hydride transfer from H_2 [3b], and therefore the introduction of H_2 into the reactor increases the observed rate of the cracking reaction. Thus, it appears that hydrogen transfer between H_2, probably activated in the zeolite, and surface carbenium ions can occur under high partial pressure of molecular hydrogen. The interaction of molecular hydrogen with intermediate carbenium ions has been studied theoretically by using the MINDO/3 method to calculate the hypersurface for the process (15): The calculation mimics a gas phase reaction, i.e., neglects adsorption of the carbocation as well as the presence of proton acceptors, and predicts that the controlling step is the breakup of the H_2 molecule to give the final alkane and H^+. In the gas phase, where no proton acceptor is present, the energy barrier for the abstraction of the proton is about 280 kJ mol^{-1}. This barrier should be much smaller on a zeolite, where H_2 is already activated and stabilized on the surface by means of the acid–base pairs, and the resulting proton will be stabilized by the anionic framework of the zeolite.

The hydride transfer from hydrogen was confirmed by the higher *P/O* ratios observed at any level of conversion on any zeolite when the reaction was carried out in hydrogen atmosphere (Fig. 3 and Tables 3 and 4).

It has to be pointed out that owing to differences in pore dimensions the hydrogen transfer from hydrocarbons and therefore the *P/O* ratio is much lower on MFI than on USY zeolites when the reaction is carried out in the presence of N_2.

With respect to the influence of the nature of active sites, the results from Table 4 show that the removal of the EFAL (samples FAU1 and FAU1F1; FAU2 and FAUF2) increases the hydrogen transfer from hydrocarbons (cracking carried out in N_2), and the hydrogen transfer from hydrogen (cracking carried out in the presence of H_2). Therefore, it is apparent that it is neither the EFAL nor the total number of framework Al which controls the extension of hydrogen transfer reactions, but the number of accessible Brønsted acid sites. In Fig. 6 the activities of the different FAU-type zeolite samples are shown as a function of the number of Brønsted acid sites. It becomes evident that the reaction is proportional to the number of these sites accessible for pyridine and so for *n*-heptane. However, it is clearly indicated that two ranges with nonequivalent catalytic proper-

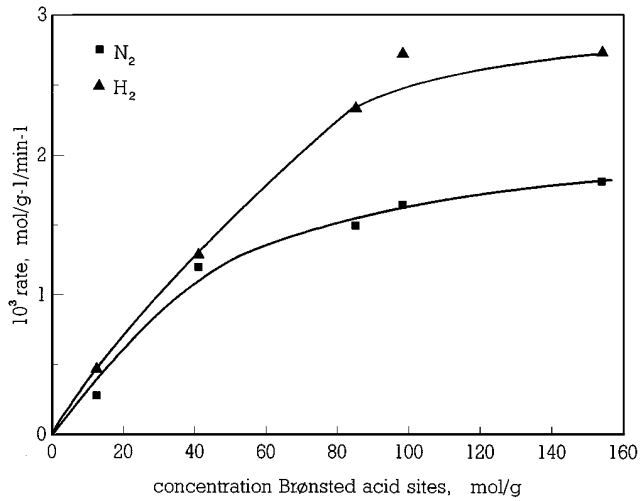

FIG. 6. Cracking rate of FAU-type zeolites dependent on concentration of OH groups determined by pyridine adsorption: temperature, 623 K; p_{total}, $p_{n\text{-heptane}}$, 0.4 MPa.

ties exist. The intrinsic activity of the Brønsted acid sites seems to be lower at concentrations of Brønsted acid OH groups higher than 80 μmol g^{-1}. This might be caused by three different reasons:

(a) In the region of Brønsted acid site concentration above 80 μmol g^{-1} there exist between 18 and 28 FAL species per unit cell, which means that between 2.25 and 3.5 Brønsted acid sites are located in one supercage. The efficiency (or turnover) of these sites might be lower owing the steric difficulty of more than one site in a supercage operating at the same time. The geometrical restrictions for hydrogen transfer with molecular hydrogen should be of less importance. However, if the reaction is carried out in hydrogen, again a lower turnover of sites in FAU-type zeolites with a site density higher than 80 μmol g^{-1} is observed.

(b) It is known that hydrogen transfer reactions are sensitive to acid site density. The formation of coke, which implies successive hydrogen transfer leading to strongly adsorbed unsaturated carbenium ions, is also likely to depend on acid site density. A more rapid fouling of the catalyst with more than 80 μmol g^{-1} Brønsted acid sites could be responsible for the observed decrease in specific activity, too. Therefore the rate of deactivation was determined for sample FAU2F and FAU1F2 (Fig. 7). It becomes evident that deactivation (definition is given later on) of sample FAU2F is faster than that of sample FAU1F2.

(c) Finally, the results can be explained by a decrease in the acid strength due to creation of AlO_4 tetrahedra with close Al neighbors in the second shell of T-positions. The enhancing effect due to the presence of hydrogen is most pronounced with samples which were assumed to have Brønsted acid sites of lower strength. Thus, one comes to the conclusion that there are Brønsted acid sites which, although not active enough to catalyze the paraffin cracking, can still adsorb olefins and hydrogen can be transferred to them. Hence, the hydrogenation reaction [3b] would obviously lead to an overall decrease of the olefin partial pressure in the gas phase and thus favor the desorption of olefins from stronger acid sites. This would mean that in general weak acid sites could support the action of strong acid sites by elimination of adsorbed olefins, which limits the overall reaction rate.

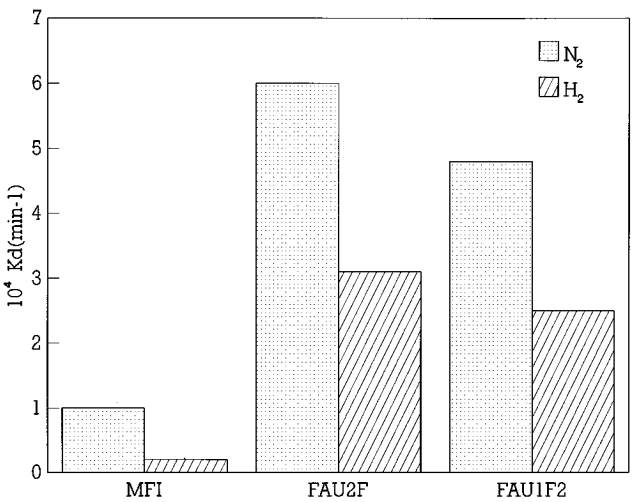

FIG. 7. Rate of deactivation during *n*-heptane cracking on MFI1, FAU2F, and FAU1F2: temperature, 623 K; p_{total}, $p_{n\text{-heptane}}$, 0.4 MPa.

Under the given experimental conditions all the investigated zeolites were able to catalyze hydrogen transfer from molecular hydrogen. Taking into account that the reverse of the proposed reaction [3b] is identical with the well-established protonation of a C–H bond in a saturated hydrocarbon (1) during protolytic cracking, this seems reasonable.

The presented results not only show the high activity of zeolites for transferring hydride ions from H_2 to surface carbenium ions but also establishes a linkage between cracking and hydroisomerization–hydrocracking. Indeed, it may happen that in the case of hydrocracking, which occurs at much higher pressures than catalytic cracking, and in the presence of H_2 and a noble metal (Pt), the enhanced activity and isomerization selectivity obtained in comparison to the monofunctional catalysts is due, at least in part, to the fast desorption of adsorbed olefinic products, owing to the presence of hydrogen, which can be activated more efficiently by the metal. The increase in the rate of desorption will decrease the average lifetime of carbenium ions, and therefore, increase the selectivity to intermediate branched isomers as well as decrease the extension of secondary reactions leading to coke and consequently to catalyst deactivation. This can be deduced from the analysis of the deactivation behavior of the two different zeolite types used during cracking at 623 K, total pressure of reaction of 2.4 MPa, and *n*-heptane partial pressure of 0.42 MPa. The model introduced by Das and Wojciechowski (16) was applied to the experimentally determined functions of relative activity versus TOS in nitrogen and hydrogen atmosphere. The fitting was executed with fixed values of all other parameters except the parameter k_D. This parameter expresses the rate of deactivation. In agreement with the literature (17, 18) the rate of deactivation was found to be higher for FAU than for MFI-type zeolites (Fig. 7), and in any case the presence of hydrogen diminishes the deactivation rate during *n*-heptane cracking. However, the presence of hydrogen during cracking does not change the relative ordering concerning zeolite deactivation.

In previous papers the deactivation was attributed to carbonaceous deposits (5, 12). Our model concerning the action of hydrogen during *n*-heptane cracking starts from the idea that hydrogen diminishes the concentration of intermediate carbenium ions, and therefore the concentration of precursors for coke formation. If this is so, hydrogen should influence mostly the amount of coke produced. In order to

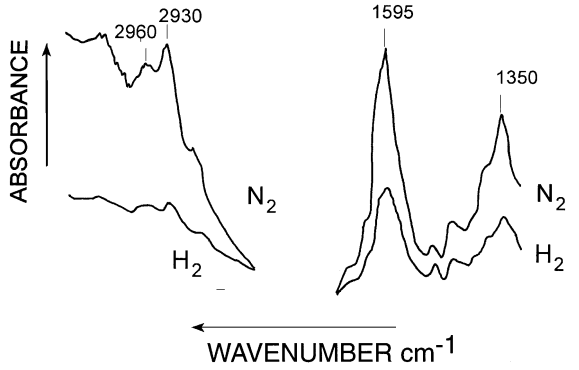

FIG. 8. IR spectra of sample FAU1 after performing *n*-heptane cracking at 0.47 MPa *n*-heptane partial pressure in nitrogen and hydrogen atmosphere: temperature, 623 K; p_{total}, 2.4 MPa.

prove this hypothesis, the catalyst FAU1 was investigated after allowing the cracking to proceed for 60 min TOS in nitrogen and hydrogen atmosphere. The reaction was followed by flushing the reactor system for a further 60 min with nitrogen. Self-supporting wafers of the zeolite samples were prepared. Before taking the IR spectra of the zeolites, they were activated at 623 K under vacuum to remove the adsorbed water. The results are given in Fig. 8 and show that the intensity of the absorption bands at 1595 and 1350 cm^{-1}, which are assigned to the presence of coke deposits (20), strongly depend on the nature of the carrier gas used. The total amount of "coke" was much lower when the reaction was performed in hydrogen atmosphere. Furthermore, it has to be pointed out that there is no indication that significant amounts of aromatic compounds (absorption at 3050 cm^{-1} (21)) have been formed during the reaction either in the presence of nitrogen or hydrogen. The deactivation seems to be caused mainly by strongly adsorbed unsaturated, aliphatic hydrocarbons. Their surface concentration is regulated by the hydrogen partial pressure present during the reaction. These results support the conclusion drawn above.

CONCLUSIONS

Under reaction conditions such as a temperature of 623 K and a total reaction pressure of 2.4 MPa, cracking of *n*-heptane proceeds preferentially according a bimolecular chain reaction mechanism on MFI- and FAU-type zeolites. Regardless of the zeolite used the bimolecular hydrogen transfer between adsorbed species and educt molecules is catalyzed and dominates the observed processes. The activity for this type of hydrocarbon conversion can be attributed to the number of Brønsted acid sites. The cracking activity increases linearly with concentration of these sites in cases where no difference in the intrinsic acidity of sites is evident. This was confirmed for MFI-type zeolites. Brønsted sites of lower acid strength cause lower specific activity in *n*-heptane cracking. Hence, FAU-type zeolites have shown lower activities for *n*-heptane cracking than MFI-type zeolites under similar reaction conditions. Furthermore. FAU-type zeolites rich in aluminium (concentration of OH higher than 80 μmol g^{-1}) exhibit lower specific activities, which becomes reasonable by assuming a lower acid strength of Brønsted acid sites for these zeolites.

Hydrogen transfer involving molecular hydrogen has taken place on all zeolite samples investigated.

This study points out that transfer of hydrogen from molecular hydrogen and from hydrocarbons occurs symbiotically. The influence of molecular hydrogen on activity and selectivity during *n*-heptane cracking allows the establishment of a link between isomerization-cracking reactions carried out on monofunctional and on bifunctional (acid plus metal) catalysts.

ACKNOWLEDGMENTS

The European Union is gratefully acknowledged for promoting cooperation, through the network CHRX-ET93-0289 (DG 12 COMA). The work of J. M. at the Instituto de Tecnología Química was supported by the Deutsche Forschungsgemeinschaft.

REFERENCES

1. Haag, W. O., and Dessau, R. M., *in* "Proceedings, 8th International Congress on Catalysis, Berlin, 1984," Vol. 2, p. 305. Dechema, Frankfurt-am-Main, 1984.
2. Giannetto, G., Pérot, G., and Guisnet, M., *in* "Proceedings, International Symposium on Zeolite Catalysis, Siófok, Hungary, 1985," p. 467.
3. Mirodatos, C., and Barthomeuf, D., *J. Catal.* **93**, 246 (1985).
4. Wielers, A. F. H., Vaarkamp, M., and Post, M. F. M., *J. Catal.* **127**, 51 (1991).
5. Meusinger, J., and Corma, A., *J. Catal.* **152**, 189 (1995).
6. Schwieger, W., Bergk, K.-H., Freude, D., Hunger, M., and Pfeiffer, H., *ACS Symp. Ser.,* 398 (1989).
7. Fichtner-Schmittler, H., Lohse, V., Engelhard, G., and Patzelová, *Cryst. Res. Technol.* **19**, 1, k1–k3 (1984).
8. Emeis, C. A., *J. Catal.* **141**, 347 (1993).
9. Barthomeuf, D., Materials Chemistry and Physics, **17**, 49 (1987).
10. Corma, A., Fornès, V., and Rey, F., *Appl. Catal.* **59**, 267 (1990).
11. Barthomeuf, D., and Beaumont, R., *J. Catal.* **30**, 288 (1973).
12. Meusinger, J., Liers, J., Mösch., A., and Reschetilowski, W., *J. Catal.* **148**, 30 (1994).
13. Petunchi, J. O., Sill, G. A., and Hall, W. K., *J. Catal.* **141**, 323 (1993).
14. Corma, A., Faraldos, M., Martinez, A., and Mifsud, A., *J. Catal.* **122**, 230 (1990).
15. Corma, A., Sanchèz, J., and Tomàs, F., *J. Mol. Catal.* **19**, 9 (1983).
16. Das, A. K., and Wojciechowski, B. W., *Chem. Eng. Sci.* **48**, 1041 (1993).
17. Walsh, D. E., Rollmann, L. D., *J. Catal.* **56**, 195 (1979).
18. Schulz, H., Böhringer, W., and Zhao, S., *in* "Proceedings, 9th International Zeolite Conference, Montreal, 1992" (R. von Ballmoos *et al.,* Eds.), Vol. 2, p. 567. Butterworth-Heinemann, Boston, 1993.
19. Jolly, S., Saussey, J., Lavalley, J. C., Zanier, N., Benazzi, E., and Joly, J. F., *in* "Proceedings, 9th International Zeolite Conference, Montreal, 1992" (R. von Ballmoos *et al.,* Eds.), Vol. 2, p. 319. Butterworth-Heinemann, Boston, 1993.
20. Espinat, D., Dexpert, H., Freund, E., Martino, G., Couzi, M., Lespade, P., and Cruege, F., *Appl. Catal.* **16**, 343 (1985).
21. Jentys, A., and Lercher, J. A., *in* "Proceedings, 8th International Zeolite Conference, Amsterdam, 1989" (P. A. Jacobs *et al.,* Eds.), Elsevier, Amsterdam, 1989; *Stud. Surf. Sci. Catal.* **49**, 585 (1989).